



HAL
open science

NIR electrochemical fluorescence switching from polymethine dyes

Seogjae Seo, Simon Pascal, Chihyun Park, Kyoungsoon Shin, Xu Yang, Olivier Maury, Bhimrao D. Sarwade, Chantal Andraud, Eunkyong Kim

► **To cite this version:**

Seogjae Seo, Simon Pascal, Chihyun Park, Kyoungsoon Shin, Xu Yang, et al.. NIR electrochemical fluorescence switching from polymethine dyes. *Chemical Science*, 2014, 5 (4), pp.1538-1544. 10.1039/C3SC53161A . hal-01288845

HAL Id: hal-01288845

<https://hal.science/hal-01288845>

Submitted on 5 Oct 2022

HAL is a multi-disciplinary open access archive for the deposit and dissemination of scientific research documents, whether they are published or not. The documents may come from teaching and research institutions in France or abroad, or from public or private research centers.

L'archive ouverte pluridisciplinaire **HAL**, est destinée au dépôt et à la diffusion de documents scientifiques de niveau recherche, publiés ou non, émanant des établissements d'enseignement et de recherche français ou étrangers, des laboratoires publics ou privés.



Distributed under a Creative Commons Attribution 4.0 International License

NIR Electrochemical Fluorescence Switching from Polymethine Dyes

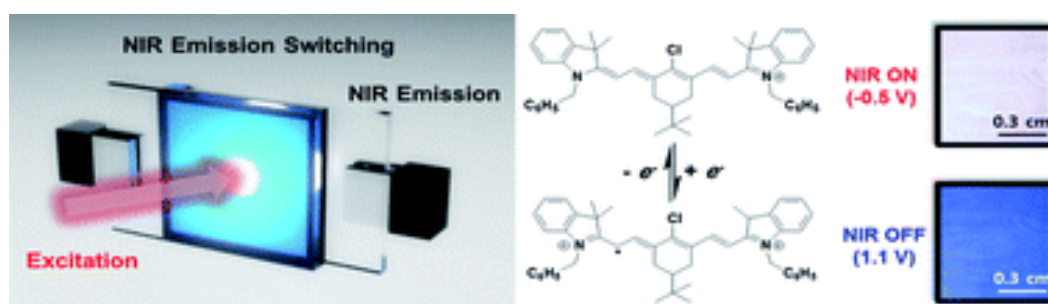
Seogjae Seo,^a Simon Pascal,^b Chihyun Park,^a Kyoungsoon Shin,^a Xu Yang,^a Olivier Maury,^b Bhimrao D. Sarwade,^a Chantal Andraud*^b and Eunkyong Kim*^a

^a Department of Chemical and Biomolecular Engineering, Yonsei University, 50 Yonsei-ro, Seodaemun-gu, Seoul 120-749, Korea

E-mail: eunkim@yonsei.ac.kr

^b Ecole Normale Supérieure de Lyon, University of Lyon, CNRS-UMR 5182, 46 Allée d'Italie, 69007 Lyon, France

E-mail: chantal.andraud@ens-lyon.fr



ABSTRACT

A polymethine dye was used as a fluorophore and an electroactive modulator in order to achieve reversible electrochemical fluorescence switching in the near infrared (NIR) region. An NIR emissive polymethine dye, 3H-indolium, 2-[2-[2-chloro-3-[2-[1,3-dihydro-3,3-dimethyl-1-(phenylmethyl)-2H-indol-2-ylidene]ethylidene]-5-(1,1-dimethylethyl)-1-cyclohexen-1-yl]ethenyl]-3,3-dimethyl-1-(phenylmethyl)-bromide (PM1), displayed high absorption and emission in the NIR region. In addition, it showed a relatively reversible electrochemical reaction between -0.5 and 1.1 V vs. Ag wire. In contrast, a keto group (C=O) bridged polymethine analogue, 2,6-bis[2-(1,3-dihydro-1-hexyl-3,3-dimethyl-2H-indol-2-ylidene)ethylidene]-4-(1,1-dimethylethyl)cyclohexanone (PM2), showed an irreversible electrochemical reaction, possibly due to the keto group interrupting the full conjugation of the entire molecule in PM2. The reversible redox reaction of PM1 allowed electrochemical fluorescence switching in the NIR region for the first time. The NIR fluorescence switching was visually observable through a visible light cut-off filter with a cyclability of over 100.

Electronic supplementary information (ESI) available. See DOI: [10.1039/c3sc53161a](https://doi.org/10.1039/c3sc53161a)

1. Introduction

Interest in stimuli-responsive fluorescence changes has grown rapidly due to a number of applications related to ion sensing,^{1,2} bioanalysis,³⁻⁵ fluorescence imaging,^{6,7} and reversible control for optical memories.^{8,9} In order to respond to these research demands, electrochemical fluorescence (EF) switching has become a promising approach, as it can provide reversible and stable fluorescence modulation based on the conversion of redox states.¹⁰⁻¹⁵ The EF switching is based on the energy transfer between the fluorophore and the electroactive acceptor, or the intrinsic fluorescence quenching of the electroactive fluorophore, so reversible electrochemistry and its correlation with fluorescence is essential to obtain measurable EF switching.^{10,13} Previous reports have employed poly(oxadiazole)s,⁷ poly(methylene-anthracene)s,¹⁶ and various tetrazine derivatives^{12,13,17-19} as materials to design reversible and stable EF switching devices. In this context, we recently reported a solid-state EF device in which a tetrazine fluorophore was blended with a solid polymer electrolyte (SPE) to form an electrofluorochromic layer.^{17,18} Furthermore, multi-color fluorescence switching was achieved by blending a naphthalimide to an electrofluorochromic layer, resulting in a white-blue-dark state of fluorescence.¹² However, attempts have not been made to extend the switchable emission to the near-infrared (NIR) spectral region, although optical properties in the NIR region have attractive advantages in bio-imaging, bio-analysis,²⁰ and night vision devices.^{21,22} Especially, in biomedical imaging, the use of NIR emission is a promising approach because it can provide non-invasive and background signal free images.²³ Based on these advantages, NIR dyes featuring absorption and emission bands in the 700–1200 nm spectral range, are currently being studied extensively due to the high interest in various applications ranging from bioimaging to NIR modulation devices and dark field viewing devices.^{24,25} Therefore, modulation of NIR emission can provide an additional functionality in imaging applications, such as selective NIR fluorescence probes,²⁶ and biomedical diagnosis.²⁷ Also, with dark field viewing application, modulation of NIR emission can lead to meaningful signaling devices, and signal perturbing devices.²⁸

Herein, we report NIR EF switching, for the first time, using an NIR emissive polymethine dye, after careful control of the redox reaction of the dyes within the working potential window. A polymethine dye was employed, because it gives fluorescence in the NIR region with the excitation of visible to NIR incident light, while they are electroactive. To investigate the relationship of chemical structure on EF switching, a cationic (PM1) and neutral polymethine dye (PM2) were examined under the same experimental conditions. Ultimately, the precise control of the applied potential resulted in optimized ON/OFF switching, while minimizing irreversible decomposition.

2. Experimental

2.1. Materials

Polymethine dyes PM1, PM2 were prepared following the previously reported procedures.^{25,29,30} [PM1: ¹H NMR (500.10 MHz, CDCl₃, δ): 8.22 (d, ³J = 14 Hz, 2H, =CH), 7.42–7.23 (m, 18H, CH_{Ar}), 6.21 (d, ³J = 14 Hz, 2H, =CH), 5.56 (d, ²J = 16.5 Hz, 2H, CH₂), 5.46 (d, ²J = 16.5 Hz, 2H, CH₂), 2.62 (dd, ²J = 16 Hz, ³J = 4 Hz, 2H, H_{eq}), 2.07 (dd, ²J = 14 Hz, ³J = 14 Hz, 2H, H_{ax}), 1.75 (s, 6H, C(CH₃)₂), 1.73 (s, 6H, C(CH₃)₂), 1.38 (m, 1H, CH), 0.99 (s, 9H, C(CH₃)₃); ¹³C NMR (125.75 MHz, CDCl₃, δ): 172.4 (C_{quat}), 150.4 (C_{quat}), 144.1 (CH), 143.0 (C_{quat}), 141.0 (CH), 134.5 (C_{quat}), 129.4 (CH), 129.1 (CH), 128.7 (C_{quat}), 128.4 (CH),

126.8 (CH), 125.5 (CH), 122.5 (CH), 111.2 (CH), 102.7 (CH), 49.4 (C_{quat}), 48.6 (N-CH₂), 42.2 (CH), 32.5 (C_{quat}), 28.4 (C(CH₃)₂), 28.3 (C(CH₃)₂), 27.7 (CH₂), 27.6 (C(CH₃)₃). UV-vis (dichloromethane): λ_{\max}/nm ($\epsilon/\text{M}^{-1} \text{cm}^{-1}$) = 795 (370 000). $\Phi_{\text{F}} = 0.29$ (IR-125 as reference, $\Phi_{\text{F}} = 0.13$ in DMSO). [PM2: ¹H NMR (500.10 MHz, CDCl₃, δ): 8.21 (d, ³J_{trans} = 13 Hz, 2H, =CH), 7.31–7.22 (m, 4H, CH_{Ar}), 6.95 (dd, ³J = 7 Hz, 2H, CH_{Ar}), 6.73 (d, ³J = 8 Hz, 2H, CH_{Ar}), 5.53 (d, ³J_{trans} = 13 Hz, 2H, =CH), 3.72 (t, ³J = 7 Hz, 4H, N-CH₂), 2.92 (d, ²J = 13 Hz, 2H, H_{eq}), 2.18 (dd, ²J = 14 Hz, ³J = 14 Hz, 2H, H_{ax}), 1.78 (t, ³J = 7 Hz, 4H, CH₂), 1.73 (s, 6H, C(CH₃)₂), 1.72 (s, 6H, C(CH₃)₂), 1.50–1.37 (m, 13H, CH₂ and CH), 1.11 (s, 9H, C(CH₃)₃), 0.96 (t, ³J = 7 Hz, 6H, CH₃-CH₂). ¹³C NMR (125.75 MHz, CDCl₃, δ): 186.5 (C_{quat}), 162.3 (C_{quat}), 144.3 (CH), 139.7 (C_{quat}), 141.1 (C_{quat}), 132.8 (CH), 127.6 (CH), 126.5 (C_{quat}), 121.8 (CH), 120.4 (CH), 106.6 (CH), 46.5 (C_{quat}), 43.6 (CH), 42.6 (N-CH₂), 32.6 (C_{quat}), 31.5 (CH₂), 28.8 (CH₃), 28.7 (CH₃), 27.5 (CH₃), 26.9 (CH₂), 26.8 (CH₂), 26.1 (CH₂), 22.6 (CH₂), 14.0 (CH₃). MS (ESI) m/z : [M + H]⁺ calc. for C₄₆H₆₅N₂O, 661.5091; found, 661.5081%. UV-vis (dichloromethane): λ_{\max}/nm ($\epsilon/\text{M}^{-1} \text{cm}^{-1}$) = 508 (52 000). $\Phi_{\text{F}} = 0.05$ (rubrene as reference, $\Phi_{\text{F}} = 0.27$ in methanol)]. Tetrabutylammonium hexafluorophosphate (TBAPF₆) and dichloromethane (MC) were obtained from Aldrich were used as a liquid electrolyte. Ag wire, which was used as a reference electrode, was purchased from Nilaco Corp. All solvents and chemicals were reagent grade and were used as purchased.

2.2. Preparation of the EF switching cells

The fluorescence switching devices consisted of an electrolyte that was packed between two ITO electrodes (13 Ωsq^{-1}), with Ag wire ($d = 0.1 \text{ mm}$) as the reference electrode. The electrolyte solution was prepared by mixing the polymethine dyes (0.01 M) in a 0.2 M concentration of TBAPF₆/CH₂Cl₂ solution. The switching device was prepared by assembling the ITO electrode, with Ag wire as the reference electrode, between the working and counter electrodes. The electrolyte was carefully injected into the device through holes drilled into the counter electrode. The holes were sealed by heating with a hot melt 25 μm -thick Surlyn polymer film (Surlyn, Solaronix Meltonix 1170-25). The device was then finally sealed with an epoxy resin.¹²

2.3. Measurements

Electrochemical measurements for the prepared EF switching cells were obtained using a universal potentiostat [model CHI 624B (CH Instruments, Inc.)]. Cyclic voltammetry (CV) and differential pulse voltammetry (DPV) were performed after 5 min of nitrogen purging. UV-vis spectra were obtained using the spectrometer Lambda 750 (PerkinElmer). Fluorescence spectra were measured using a Model LS55 luminescence spectrometer (PerkinElmer). NIR photography was obtained with a digital camera (IR cut-off filter removed, Power Shot A640, Canon) with a visible light cut-off filter (720 nm, 830 nm cut-off filter), and with 785 nm excitation source (optical power = 3 mW, Su Semiconductor, Korea). The light intensity of the excitation source was determined by dividing the optical power by the irradiation area. When recording the fluorescence along with the external voltage, the *in situ* fluorescence of the switching device was obtained using a luminescence spectrometer.

3. Results and discussion

3.1. Optical and electrochemical properties of the polymethine dyes

The optical properties of polymethine dyes were well matched with the previous report.²⁵ The cationic polymethine dye (PM1) was well soluble in organic solvents and showed a green color in solution. The absorption and fluorescence bands were maximized in the NIR spectral range, as expected from the long electron delocalization between the two electron-donating groups through the hydrocarbon skeleton.³¹ The maximum absorption band for PM1 was observed at 795 nm with an extremely high extinction coefficient of $370\,000\text{ L mol}^{-1}\text{ cm}^{-1}$ (Fig. 1). The fluorescence appeared as a sharp band in the NIR region and maximized at 822 nm. The absorption and emission colors in the NIR region for PM1 were almost imperceptible without the aid of the visible light cut-off filters. On the other hand, a neutral polymethine dye (PM2) showed a pale red hue when dissolved in dichloromethane, showing an absorption maximum at 508 nm with an extinction coefficient of $52\,000\text{ L mol}^{-1}\text{ cm}^{-1}$, (Fig. 1). This absorption resulted in a bright fluorescence band in the visible range (maximum at 555 nm). Because PM2 is a neutral polymethine dye with an electron-donating indole group, the absorption band appears at a shorter wavelength region compared to PM1. Ketocyanines, such as PM2 can be easily protonated in acidic media, leading to a cationic dyes exhibiting intense and red-shifted absorption.^{29,30,32}

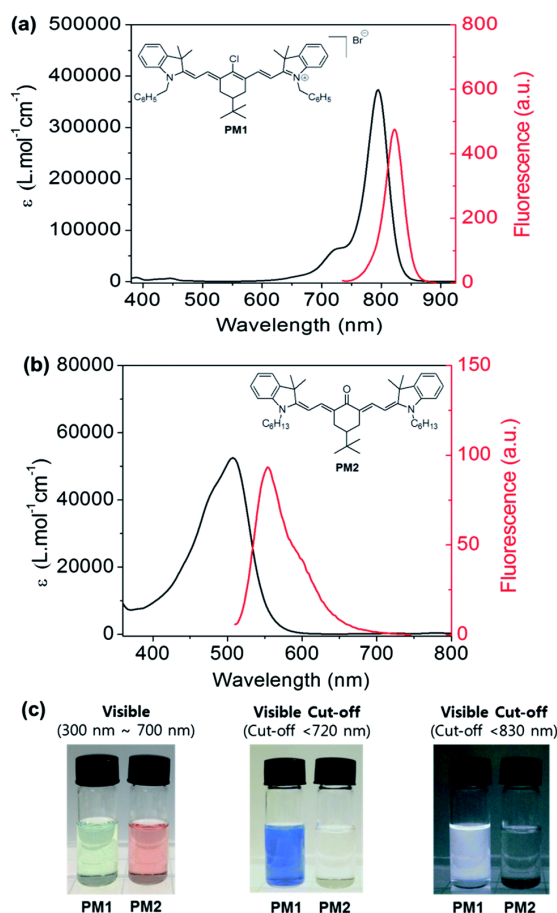


Fig. 1 Absorption (black line) and fluorescence (red line) spectra of solutions for (a) PM1 and (b) PM2 in dichloromethane. (c) Photographic images of the polymethine dyes with the visible and visible cut-off optical filters (dye conc. = $2 \times 10^{-6}\text{ M}$, in dichloromethane).

The transparent green and red solution of PM1 and PM2, respectively, are shown in the photographic images of [Fig. 1c](#), which were obtained under room light with a normal camera without visible light cut-off filters. With the aid of a visible cut-off filter, the absorption and emission of the PM1 solution became visible. The NIR images obtained by the digital camera through the cut-off filter with a cut-off <720 nm and <830 nm displayed vivid blue and bright white color, respectively, for the PM1 solution. As the digital camera presents a processed image, which is white-balanced using a white background, the colors of the output image possibly indicates the color from the transmitted light out of the detectable light. Therefore, the blue color of the PM1 solution ([Fig. 1c](#), with a < 720 nm cut-off) indicates that the light near 780 nm is absorbed by PM1, and the light near 720 nm is transmitted. With an <830 nm cut-off filter, it appeared that the detectable wavelength was limited by the filter and detection limit of the CCD. Interestingly, the image obtained by the greyscale image presented the bright emission of PM1 under room light, as the absorption band of PM1 was in the cut-off region. This is similar to the NIR fluorescence imaging systems used in biotechnology, which are equipped with excitation sources and NIR band-pass filters.^{33,34} Our system provides a simpler method to obtain convertible NIR images with various wavelength ranges. With the same conditions, the NIR image of the PM2 solution was clearly transparent through the visible cut-off filters because the absorption band of PM2 was transparent in the NIR range.

In order to elicit reversible electrochemical switching of the fluorescence for the polymethine dyes, we determined a working potential window, *i.e.*, the reversible redox potential range, through CV. The redox peaks of PM1 were matched with typical cationic polymethine dyes.³⁵⁻³⁷ Typical cationic polymethine dyes show a one-electron oxidation process that generates the corresponding radical dications (Dye²⁺). However, the radical dication is known to be irreversibly generated since it undergoes decomposition reactions such as dimerization,^{35,36} and dehydrogenation.^{38,39} These decomposition reaction could be partially inhibited in PM1 due to the electronic stabilization by the extended conjugation, and by steric hindrance.^{36,40,41} To minimize such decomposition process, it is necessary to apply potentials within the reversible electrochemical switching range, as described below.

[Fig. 2a](#) shows the CV of PM1, which undergoes a redox reaction with the same mechanism as the general polymethines. The partially reversible one-electron oxidation process was observed at 0.94 V, in which the ratio for the reduction/oxidation current densities was 0.84, as determined by the DPV method. Because the DPV technique is designed to minimize background currents, DPV curves can be used in quantitative analysis. The amounts of the unrecovered electrons may represent the quantities of the decomposed radical dications during the oxidation process. Although the oxidation process was not completely reversible, it is more reversible when compared to other carbocyanine dyes.^{40,41} This characteristic can be explained by the molecular structure of PM1. As the molecular structure of PM1 is significantly crowded by a *tert*-butyl group and a phenyl group, the steric hindrance by such groups would make PM1 have a high resistance toward the decomposition. On the other hand, a partially reversible reduction wave appears at -0.35 V, which is probably due to the reduction of the methine group. Because the neutral radicals for most polymethine dyes are generally more active than radical dications,^{35,36} the ratio for the reduction/oxidation current densities was smaller than the oxidation process ($r = 0.65$). The low current density observed in the reduction process may be attributed to the decomposition of the neutral radical in the non-flow electrochemical system.^{40,41} The reversibility of the oxidation and reduction process for PM2 was quite different from PM1, as shown in [Fig. 2b](#). Specifically, the oxidation process to generate the radical cation ($E_p = 0.62$ V) is much more irreversible with a reduction/oxidation current area ratio of 0.25, with the same experimental conditions as those for PM1. The reduction process observed at

−0.98 V was quite weak and irreversible. These differences can be attributed to the different conjugation of the methine chain induced by the keto group (C=O).^{42,43} Therefore, the reversible redox potential ranges, with minimum electrochemical decomposition, were −0.5 to 1.1 V and −1.1 to 0.7 V for PM1 and PM2, respectively. CV was performed with this optimum range, along with a fast scan rate to avoid any side reactions.

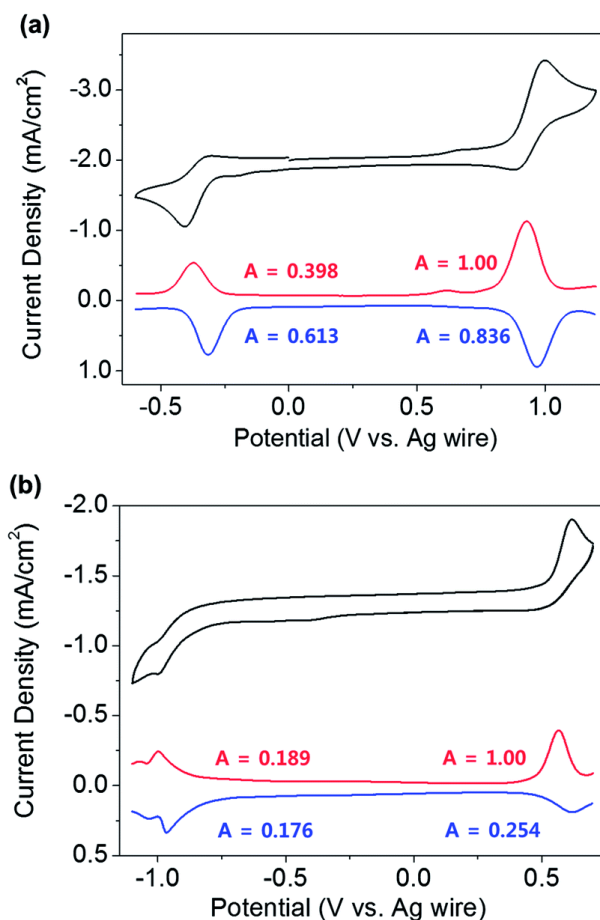


Fig. 2 Cyclic voltammogram of (a) PM1 and (b) PM2 in an electrolyte containing TBAPF₆ 0.2 M as salt in dichloromethane. The fluorophores were measured in a solution state of 10^{−3} M concentration in the electrolyte, with Ag wire reference electrode, and Pt disk working electrode (scan rate = 100 mV s^{−1}). The differential pulse voltammograms (DPV) were measured using the same electrolyte. The DPV was acquired using a 50 ms pulse width, 50 mV amplitude, 200 ms pulse period, and 4 mV potential increment (overall scan rate = 20 mV s^{−1}). The area of the current peak was normalized with respect to the area of the first oxidation process.

3.2. EF switching of the polymethine dyes

For the switching device, the applied potential was carefully controlled in order to achieve a reversible conversion. With a three-electrode device, using Ag wire as a reference electrode, the applied potential could be precisely controlled to avoid the degradation that occurs as a result of over-potential.^{7,10,12} Although Ag wire is not a stable reference electrode, it can provide a simple three-electrode system in flat electrochemical devices. Also, through the precise potential control, the applied potential at the counter electrode can be minimized to exclude side electrochemical reactions. In Fig. S1,[†] the redox potential of ferrocene was measured with Ag wire reference electrode to calibrate the redox potential. Fig. 3 shows the fluorescence spectra at different applied potentials for the three-electrode device that contains PM1. With a 733 nm excitation, a characteristic NIR emission for PM1 was observed in the

820 nm region. The emission peak was shifted slightly, possibly due to a high concentration. Interestingly, the intensity of the fluorescence gradually decreased with the oxidation from -0.4 to 1.1 V, without any peak shifts. This indicates that the fluorescence quenching originated from the electrochemical oxidation of PM1, from the cation to the radical dication. This was clearly shown in the cyclic electrochemical fluorescence spectra (Fig. 3b). The fluorescence intensity of PM1 started to decrease at ~ 0.8 V, which exactly matches the onset potential of the one-electron oxidation. Similar to the redox band, the fluorescence was quenched gradually through the generation of the radical dication, and was then recovered with a reduction sweep. Interestingly, only $\sim 30\%$ of the quenched fluorescence was recovered when the potential sweep returned to 0 V, where the generated radical dication of PM1 should be reversibly converted to its original cation state. This loss was recovered at a potential below -0.25 V, which is the onset potential for the electro-conversion to the neutral radical. A possible explanation for this unusual fluorescence recovery is presented as follows. Considering the electrochemistry of a typical polymethine dye, $\text{Dye}^{\cdot 2+}$ could be generated with an oxidation sweep, resulting in fluorescence quenching. However, the reverse reaction seems unfavorable to the formation of some remaining $\text{Dye}^{\cdot 2+}$, as shown in CV and the electrochemical fluorescence spectra. This may also contribute to the low current density for the reduction process (-0.35 V), which is $\sim 50\%$ smaller than the oxidation process (0.94 V). Moreover, with the reduction sweep, the neutral radical (Dye^{\cdot}) could be generated on the working electrode, which is known to be more active than the radical dication. Therefore, with some excited energy, the reaction between the remaining $\text{Dye}^{\cdot 2+}$ and Dye^{\cdot} should be a favorable reaction to the formation of Dye^+ . In fact, this process is similar to the mechanism of electrochemical luminescence, where the collision between $\text{Dye}^{\cdot 2+}$ and Dye^{\cdot} is used to generate luminescence.^{39,44,45} Furthermore, the electrochemical luminescence property of a polymethine derivative was demonstrated in the previous report.³⁹ Therefore, this could be a reasonable explanation for the secondary fluorescence recovery.

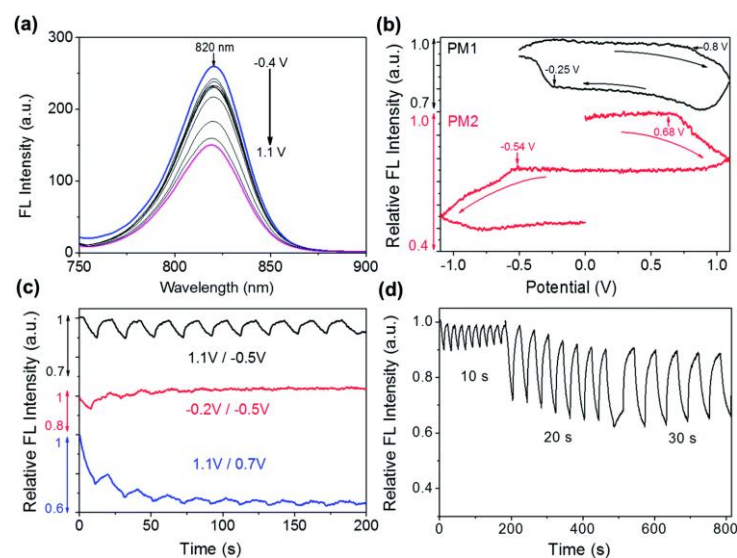


Fig. 3 (a) Fluorescence changes in the switching device containing PM1 at different applied potentials, ranging from -0.4 V (top) to 1.1 V (bottom), with a decrease of 0.1 V at each step ($\lambda_{\text{exc}} = 733$ nm). Each spectrum was obtained after applying a target potential for 10 s in order to obtain the fluorescence spectra at an equilibrated state. (b) The cyclic electrochemical fluorescence spectra of PM1 and PM2, which recorded the fluorescence peak intensity with a scan rate of 10 mV s^{-1} . (c) The fluorescence switching responses of the device with PM1 at different switching potentials (1.1 V/ -0.5 V, -0.2 V/ -0.5 V and 1.1 V/ 0.7 V), with a 10 s step duration time. (d) The fluorescence switching responses of the device with PM1 at various step duration times of 10 s, 20 s, and 30 s at each potential, with a switching potential of 1.1 V/ -0.5 V, monitored at 820 nm ($\lambda_{\text{exc}} = 733$ nm).

With the secondary recovery to the original state, the reversibility of PM1 was significantly increased, upon application of potentials ranging from -0.5 to 1.1 V. In order to achieve reversible and stable EF switching, the reduction process to a neutral radical was essentially required, as shown in [Fig. 3c and d](#). With the application of oxidation potential (1.1 V/ 0.7 V), the fluorescence quenching and recovery were not balanced, possibly due to the reason stated above. In addition, the fluorescence quenching was not observed with the application of reduction redox potential (-0.2 V/ -0.5 V), because the fluorescence quenching is mainly related to the stability of the $\text{Dye}^{\cdot 2+}$ state. In [Fig. 3d](#), the fluorescence responses with different potential step duration times are shown. According to the applied potential duration, the fluorescence emission contrasts became larger when the duration times at each potential step were longer, with an ON/OFF ratio varying from 1.5 to 1.2 . The maximum ON/OFF contrast reached ~ 1.5 , with a 30 s potential step and fluorescence cyclability showing reversible switching continuing for over 100 cycles with $\sim 30\%$ loss ([Fig. S2†](#)). Because this ON/OFF switching is based on the oxidation of PM1, the amount of injected/ejected charge during the switching should be quantitatively related with the oxidation of PM1. As described in the supporting information, the amount of oxidized PM1 was calculated as $\sim 11\%$ against the whole amount of PM1 in the device ([Fig. S3†](#)). Although the conversion from Dye^+ to $\text{Dye}^{\cdot 2+}$ was not completed within 20 s, the vivid NIR fluorescence switching was observed, so this indicates that the switching is driven by the formation of $\text{Dye}^{\cdot 2+}$ within the electrode diffusion layer.¹²

On the other hand, for PM2, EF switching was hardly observed because of the unavoidable electrochemical decomposition, possibly originating from the decomposition of the radical dication at 0.62 V. When PM2 was examined with the cyclic electrochemical fluorescence spectra, the intensity decreased gradually with the oxidation process, which matched the CV result ([Fig. 3b](#)). However, unlike PM1, the decreased fluorescence was not recovered with the reduction sweep, and subsequently decreased with the potential beyond reduction to the neutral radical state, as shown in [Fig. 3b](#) and [S4.†](#) Similar to the previous causes, the keto group ($\text{C}=\text{O}$) of PM2 may cause an irreversible electroconversion to lead to irreversible fluorescence quenching. Possibly due to the irreversible reaction, in the quantitative analysis, the amount of injected/ejected charge during the switching was gradually decreased ([Fig. S3†](#)). The amount of oxidized PM2 at first switching step was calculated as 24% of the whole PM2 in the device. Because PM1 was reversibly switched by 11% of the total amount of PM1, the extra injected/ejected charge in PM2 would lead to the irreversible decomposition.

Ultimately, we fabricated a reversible NIR EF switching device in a three-electrode system, and we achieved NIR intensity modulation by precisely controlling the working potential of the reversible redox reaction for PM1 ([Fig. 4](#)). Upon exposure to a laser light source (785 nm), the switching device showed fluorescence in the NIR range. This NIR emission was passed through an optical filter to remove background light and was thus pictured by a digital camera. The electrode of the device was connected to a potentiostat in order to control the applied potential ([Fig. S5†](#)). The images in [Fig. 4c](#) present the NIR switching results from the device containing PM1. The device showed the same vivid blue color (with <720 nm cut-off) and bright white color (with <830 nm cut-off) emissions seen from the PM1 solution. This emission was controlled reversibly by an applied potential, based on electrochemical conversion between the cation to the radical dication, as shown in [Fig. 4d](#). This process was reversible for over 100 cycles, but fluorescence loss was also observed due to side reactions. Although the fluorescence contrast and cyclability of PM1 were relatively smaller than other EF switching devices working in the visible range,^{12,15,17} EF switching of the NIR region was observed here for the first time with PM1.

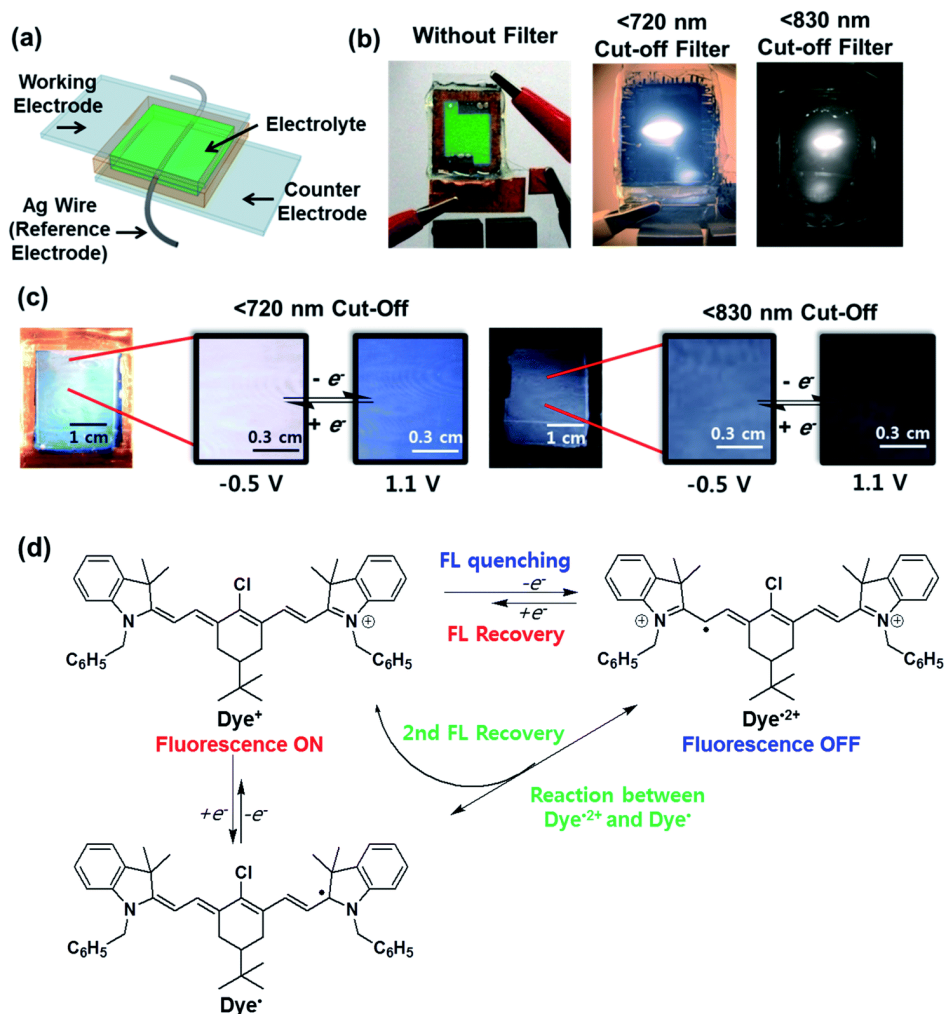


Fig. 4 (a) Schematic diagram of the EF switching device, which consists of a working electrode, counter electrode, Ag wire and NIR emissive electrolyte. (b) The photographs of the actual devices were obtained with different wavelength cut-off filters under spot excitation ($\lambda_{\max} = 785 \text{ nm}$, 5 mW cm^{-2}). (c) The ON/OFF fluorescence images were captured with <720 nm and <830 nm cut-off filters, with different applied potentials, under a diffuse NIR light ($\lambda_{\max} = 785 \text{ nm}$, 0.6 mW cm^{-2}). (d) The possible mechanism for EF switching of PM1.

4. Conclusions

In summary, we have demonstrated the electrochemical switching of NIR fluorescence for the first time, using a polymethine dye (PM1). To investigate the relations between the chemical structures of polymethine dyes and their optical and electrochemical properties, NIR emissive

PM1 was compared with a keto group (C=O) substituted analogue (PM2). Due to the conjugation of the methine chain, PM1 showed NIR emissions, under reversible electrochemical reactions. With an applied potential, PM1 undergoes oxidation to a radical dication (Dye^{•2+}) and reduction to a neutral radical (Dye[•]). Although the radical dication is known to be unstable, because of its possible decomposition reaction such as dimerization and dehydrogenation, PM1 exhibited reversible electrochemical conversion arising from the steric hindrance of the bulky substituent and the reversible reactions between Dye^{•2+} and the neutral radical Dye[•]. This is in contrast to the electrochemistry of PM2, which showed irreversible electrochemical reactions due to the conjugation break of the polymethine chain by the keto group (C=O). A stable electroconversion of PM1 was applied in EF switching. The device

showed NIR fluorescence switching with an ON/OFF ratio of ~ 1.5 and a cyclability of ~ 100 cycles. These values were relatively small compared to other EF switching systems, but modulation of the NIR fluorescence was achieved for the first time through precise control of the redox reactions of polymethine dye. We believe that further modification, following this pioneering work, can improve the contrast and cyclability significantly. This would be an interesting goal to realize highly reversible NIR modulating devices based on reversible electrochemical conversion.

Acknowledgements

This work was supported by the National Research Foundation of Korea (NRF) grant funded by the Korea government (MSIP), through the Active Polymer Center for Pattern Integration (R11-2007-050-00000-0) and Converging Research Center Program, by the Ministry of Education, Science, and Technology (2010K001430).

Notes and references

1. Y. You and S. Y. Park , *Adv. Mater.*, 2008, **20** , 3820 —3826.
2. J. You , J. Kim , T. Park , B. Kim and E. Kim , *Adv. Funct. Mater.*, 2012, **22** , 1417 —1424.
3. Y.-Q. Sun , J. Liu , X. Lv , Y. Liu , Y. Zhao and W. Guo , *Angew. Chem., Int. Ed.*, 2012, **51** , 7634 —7636.
4. Y. Wang , B. Yan and L. Chen , *Chem. Rev.*, 2013, **113** , 1391 —1428.
5. T. Behnke , J. E. Mathejczyk , R. Brehm , C. Würth , F. Ramos Gomes , C. Dullin , J. Napp , F. Alves and U. Resch-Genger , *Biomaterials*, 2013, **34** , 160 —170.
6. Y. Kim , H.-y. Jung , Y. H. Choe , C. Lee , S.-K. Ko , S. Koun , Y. Choi , B. H. Chung , B. C. Park , T.-L. Huh , I. Shin and E. Kim , *Angew. Chem., Int. Ed.*, 2012, **51** , 2878 —2882.
7. S. Seo , Y. Kim , J. You , B. D. Sarwade , P. P. Wadgaonkar , S. K. Menon , A. S. More and E. Kim , *Macromol. Rapid Commun.*, 2011, **32** , 637 —643.
8. C. Yun , J. You , J. Kim , J. Huh and E. Kim , *J. Photochem. Photobiol., C*, 2009, **10** , 111 —129.
9. C. Yun , S. Seo and E. Kim , *J. Nanosci. Nanotechnol.*, 2010, **10** , 6850 —6854.
10. S. Seo , H. Shin , C. Park , H. Lim and E. Kim , *Macromol. Res.*, 2013, **21** , 284 —289.
11. S. Seo , C. Allain , J. Na , S. Kim , X. Yang , C. Park , J. Malinge , P. Audebert and E. Kim , *Nanoscale*, 2013, **5** , 7321 —7327.
12. S. Seo , Y. Kim , Q. Zhou , G. Clavier , P. Audebert and E. Kim , *Adv. Funct. Mater.*, 2012, **22** , 3556 —3561.
13. P. Audebert and F. Miomandre , *Chem. Sci.*, 2013, **4** , 575 —584.
14. K. Nakamura , K. Kanazawa and N. Kobayashi , *Chem. Commun.*, 2011, **47** , 10064 —10066.
15. J. Yoo , T. Kwon , B. D. Sarwade , Y. Kim and E. Kim , *Appl. Phys. Lett.*, 2007, **91** , 241107.
16. J. You , Y. Kim and E. Kim , *Mol. Cryst. Liq. Cryst.*, 2010, **520** , 128 —135.
17. Y. Kim , E. Kim , G. Clavier and P. Audebert , *Chem. Commun.*, 2006, 3612.
18. Y. Kim , J. Do , E. Kim , G. Clavier , L. Galmiche and P. Audebert , *J. Electroanal. Chem.*, 2009, **632** , 201 —205.
19. C. Quinton , V. Alain-Rizzo , C. Dumas-Verdes , G. Clavier , F. Miomandre and P. Audebert , *Eur. J. Org. Chem.*, 2012, 1394 —1403.

20. J. Yang , J. Choi , D. Bang , E. Kim , E.-K. Lim , H. Park , J.-S. Suh , K. Lee , K.-H. Yoo , E.-K. Kim , Y.-M. Huh and S. Haam , *Angew. Chem., Int. Ed.*, 2011, **50** , 441 — 444.
21. D. Hertel , H. Marechal , D. A. Tefera , F. Wensheng and R. Hicks , *Intelligent Vehicles Symposium, 2009* , IEEE, 2009, pp. 273–278.
22. K.-T. Lin , S.-C. Tseng , H.-L. Chen , Y.-S. Lai , S.-H. Chen , Y.-C. Tseng , T.-W. Chu , M.-Y. Lin and Y.-P. Lu , *J. Mater. Chem. C*, 2013, **1** , 4244 —4251.
23. S. Kim , Y. T. Lim , E. G. Soltesz , A. M. De Grand , J. Lee , A. Nakayama , J. A. Parker , T. Mihaljevic , R. G. Laurence and D. M. Dor , *Nat. Biotechnol.*, 2003, **22** , 93 —97.
24. Y. Morel , A. Irimia , P. Najechalski , Y. Kervella , O. Stephan , P. L. Baldeck and C. Andraud , *J. Chem. Phys.*, 2001, **114** , 5391 —5396.
25. P.-A. Bouit , G. Wetzels , G. Berginc , B. Loiseaux , L. Toupet , P. Feneyrou , Y. Bretonnière , K. Kamada , O. Maury and C. Andraud , *Chem. Mater.*, 2007, **19** , 5325 —5335.
26. Z. Guo , S. Nam , S. Park and J. Yoon , *Chem. Sci.*, 2012, **3** , 2760 —2765.
27. X. Wu , S. Chang , X. Sun , Z. Guo , Y. Li , J. Tang , Y. Shen , J. Shi , H. Tian and W. Zhu , *Chem. Sci.*, 2013, **4** , 1221 —1228.
28. R. I. Hogg and G. S. Edwards , 1995 .
29. M. Puyol , C. Encinas , L. Rivera , S. Miltsov and J. Alonso , *Sens. Actuators, B*, 2006, **115** , 287 —296 .
30. L. Strekowski , J. C. Mason , M. Say , H. Lee , R. Gupta and M. Hojjat , *Heterocycl. Commun.*, 2005, **11** , 129 —134.
31. P.-A. Bouit , C. Aronica , L. Toupet , B. Le Guennic , C. Andraud and O. Maury , *J. Am. Chem. Soc.*, 2010, **132** , 4328 —4335.
32. M. Puyol , S. Miltsov , Í. Salinas and J. Alonso , *Anal. Chem.*, 2002, **74** , 570 —576.
33. S. Ke , X. Wen , M. Gurfinkel , C. Charnsangavej , S. Wallace , E. M. Sevic-Muraca and C. Li , *Cancer Res.*, 2003, **63** , 7870 —7875.
34. S. Kim , Y. T. Lim , E. G. Soltesz , A. M. De Grand , J. Lee , A. Nakayama , J. A. Parker , T. Mihaljevic , R. G. Laurence , D. M. Dor , L. H. Cohn , M. G. Bawendi and J. V. Frangioni , *Nat. Biotechnol.*, 2003, **22** , 93 —97.
35. S. K. Lee , M. M. Richter , L. Strekowski and A. J. Bard , *Anal. Chem.*, 1997, **69** , 4126 —4133.
36. J. R. Lenhard and A. D. Cameron , *J. Phys. Chem.*, 1993, **97** , 4916 —4925.
37. J. E. H. Buston , F. Marken and H. L. Anderson , *Chem. Commun.*, 2001, 1046 —1047.
38. J. L. Lyon , D. M. Eisele , S. Kirstein , J. P. Rabe , D. A. Vanden Bout and K. J. Stevenson , *J. Phys. Chem. C*, 2008, **112** , 1260 —1268.
39. E. K. Walker , D. A. Vanden Bout and K. J. Stevenson , *J. Phys. Chem. C*, 2011, **115** , 2470 —2475.
40. J. Lenhard and R. Parton , *J. Am. Chem. Soc.*, 1987, **109** , 5808 —5813.
41. R. Parton and J. Lenhard , *J. Org. Chem.*, 1990, **55** , 49 —57.
42. L. M. Yagupolskii , V. N. Petrik and Y. L. Slominskii , *Tetrahedron Lett.*, 2002, **43** , 3957 —3959.
43. S. Miltsov , C. Encinas and J. Alonso , *Tetrahedron Lett.*, 2001, **42** , 6129 —6131.
44. V. Balzani , A. Juris , M. Venturi , S. Campagna and S. Serroni , *Chem. Rev.*, 1996, **96** , 759 —834.
45. J. P. Sauvage , J. P. Collin , J. C. Chambron , S. Guillerez , C. Coudret , V. Balzani , F. Barigelletti , L. De Cola and L. Flamigni , *Chem. Rev.*, 1994, **94** , 993 —1019.